ELSEVIER

Chemical Engineering Journal 123 (2006) 53–58

Chemical Engineering Journal

www.elsevier.com/locate/cej

Mass transfer correlation of simultaneous removal by cementation of nickel and cobalt from sulphate industrial solution containing copper
Part II: Onto zinc powder

A. Dib, L. Makhloufi *

Laboratoire de Technologie des Matériaux et de Génie des Procédés (L.T.M.G.P), Département de Génie des Procédés, Université de Bejaïa, 06000 Bejaïa, Algeria

Received 3 October 2005; received in revised form 7 June 2006; accepted 30 June 2006

Abstract

This work is devoted to a kinetic and mass transfer study of simultaneous cementation of nickel and cobalt on zinc powder through stirred tank reactor. The influence of different parameters (stirring rate, temperature, zinc dust quantity, concentration of zinc and copper) on the process of cementation of cobalt and nickel in similar conditions to those of industrial zinc sulphate solution was experimentally determined. These parameters were studied for their effect on the rate of simultaneous cementation represented by the product $\bar{k}a_e$, of the overall mass transfer coefficient $\bar{k}$ and the effective surface area a_e. Some of the significant results are the following:

(1) The cementation reaction of nickel was found to proceed with two different rates: an initial fast rate followed by a final slower one. The product $\bar{k}a_e$ was calculated and the values increased with stirring rate and less affected by temperature. Mechanistic study of the reaction through activation energy determination ($13\,\mathrm{kJ\,mol^{-1}}$) showed that the cementation of nickel on zinc is a diffusion controlled reaction.

(2) The temporal evolution of the cobalt concentration has revealed that the re-dissolution of cobalt occurred after about 50 min. The reaction of cobalt was found under chemical control.

Keywords: Cementation; Nickel; Cobalt; Zinc powder; Kinetic; Mass transfer

1. Introduction

During the electrowinning stage of hydrometallurgical zinc production, the basic problem related to the quality of the deposited metal and the energy costs of the process is the deleterious effect of small amounts of more noble metals, for example: Ni, Co, Cu, etc. These metal impurities, which are more precious than zinc, can influence the purity of the cathode sediment through co-sedimentation and facilitate the reverse dissolution of zinc [1] by forming microgalvanic cells Zn–Ni and Zn–Co [2–5]. Therefore, adequate purification of the zinc electrolyte before electrowinning is essential. Cementation is widely used in zinc hydrometallurgy during the purification of zinc sulphate solutions. Nickel and cobalt removal by cementation in zinc hydrometallurgy is carried out at 60–90 °C in the presence of copper in solution which improves this process [1,2,5–8] and references citations contained in reference [8]. The rate of this process depends on the structure of the metal deposits formed on the surface of the cementation agent particles [4,9–11]. Few investigations have appeared on the simultaneous cementation of nickel and cobalt [1,2] by suspended zinc particles and main part of these data refers to the temporal evolution of the concentration. In this context we have studied the global kinetic of simultaneous nickel and cobalt cementation and the global mass transfer in the reactor by developing mass transfer correlations.

2. Experimental

The experimental set-up used in the experiments is shown in Fig. 1. It consisted of $1\,\mathrm{dm^3}$ cylindrical glass reactor (1) lined with a cylindrical stainless steel agitator (2) of 34.5 cm

---

* Corresponding author. Tel.: +213 34 21 57 04; fax: +213 34 21 57 04.
E-mail address: laid_mak@yahoo.fr (L. Makhloufi).

1385-8947/$ – see front matter © 2006 Elsevier B.V. All rights reserved.
doi:10.1016/j.cej.2006.06.020

Nomenclature

a	specific geometrical surface area (relate to solution density) (cm^{-1})
a_e	specific effective surface area (relate to solution density) (cm^{-1})
C	cobalt and nickel concentration at time t ($mg\,l^{-1}$)
C_0	initial concentration of nickel and cobalt ($mg\,l^{-1}$)
$\bar{d}_p$	average zinc particles diameter (cm)
D	nickel-ion diffusivity ($cm^2\,s^{-1}$)
D_R	diameter of cylindrical glass reactor
$\bar{k}$	overall mass transfer coefficient ($cm\,s^{-1}$)
$\hat{k}$	overall apparent mass transfer coefficient ($cm\,s^{-1}$)
Re_k	Reynolds number ($\sigma^{1/3}\bar{d}_p^{4/3}/\upsilon$)
Sh	Sherwood number ($\hat{k}\bar{d}_p/D$)
Sc	Schmidt number (υ/D)
t	time (min)
T	temperature (°K)
V	volume of solution (cm^3)

Greek letters

Ω	angular velocity of the agitator ($rad\,s^{-1}$)
σ	power dissipate ($N_p\bar{d}_p^5\Omega^3/V$)
υ	solution cinematic viscosity ($cm^2\,s^{-1}$)

long and of 0.6 cm diameter with four pales (each pale dimensions were 2 cm × 0.8 cm). The back surface of the agitator and pales facing the container wall was isolated with epoxy resin. The impeller was mounted centrally at a distance of $D_R/7$ from the vessel bottom, where D_R is the diameter of the cylindrical glass reactor. Also, it was connected to a variable speed motor shaft (3). The adjusted rotational speed of the stirrer was measured by an optical tachometer. The cylindrical glass reactor and its contents were immersed in a rectangular water bath to control the temperature (4). The cementation process using a zinc dust particles (5) of 0.7 mm in average diameter was investigated at experimental conditions described previously [8], i.e., the industrial solution corresponds to the average content of the main components within the following limits: Zn 160 $g\,l^{-1}$, Cu 200 $mg\,l^{-1}$, Co 10 $mg\,l^{-1}$, Ni 1.5 $mg\,l^{-1}$, Sb 0.5 $mg\,l^{-1}$, pH 2.5 ± 0.5. In the whole series of experiments, we have adjusted antimony content in the electrolyte to satisfy the condition that the ratio $Q_{Co}/Q_{Sb} = 1{:}1$ [1]. Some authors put forward the fact that ratio Co:Sb = 1:1 is a necessary permanent factor for satisfactory results during cementation [1].

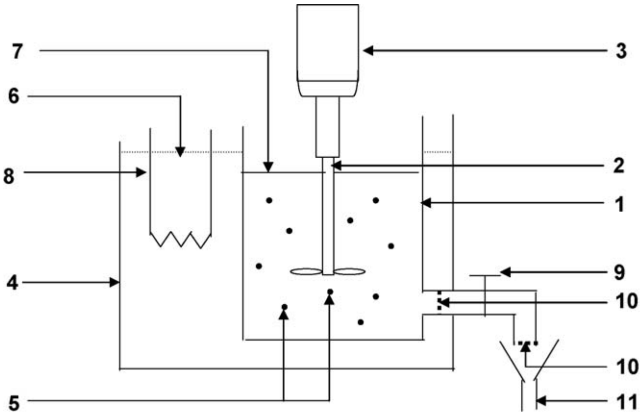

Fig. 1. Experimental apparatus used during the cementation process: (1) cylindrical glass reactor, (2) agitator, (3) variable speed motor, (4) rectangular water bath, (5) suspended zinc particles, (6) water level, (7) suspended level, (8) thermostat, (9) stopcock, (10) filter and (11) aliquots of samples.

At intervals of times, a sample of 2 cm^3 of the solution was taken, filtered and the filtrate was analysed for Ni and Co content. The analysis was performed by means of a computer controlled an atomic absorption spectrophotometer (Shimadzu AA 6500). The analyses were conducted with an oxidizing air–acetylene flame at 232 and 240.7 nm wavelengths for nickel and cobalt, respectively.

3. Results and discussion

3.1. Kinetics results

Concentration at time t (C) and initial concentration (C_0) were used to characterise the simultaneous nickel and cobalt cementation kinetics. A typical variation of log (C/C_0) with time t obtained for different experimental conditions are given in Fig. 2a and b. In all experiments the temporal evolution of the nickel concentration (Fig. 2a) exhibit two rate regions after the transition period that is approximately 5 min: a fast initial period and a final slower one. This behaviour of different reaction rates during the cementation process was observed earlier [8,12–16]. In contrast to the present results Lee et al. [12] reported a slow initial rate followed by a period of enhanced reaction using rotating zinc disc. They attributed this behaviour to the formation of a porous layer which increased the roughness of the surface and, hence, the degree of turbulence leading to an increase in the mass transfer rate. Dib and Makhloufi [8,14] and Nadkarni and Wadsworth [13] reported a decrease in the rate of cementation and attributed this decrease to the formation of a solid layer on the surface. This last view is probably more pronounced on the smaller area particles where formation of coherent non-porous precipitate is likely to occur and consequently reduces the rate of mass transfer to the surface of the particles as it is found in this work too.

It is seen that in the course of time (Fig. 2b) the concentration of cobalt reaches its minimal values after a period of time of 50–60 min, but after that they begin to increase again. These results show the reverse dissolution of metallic cobalt cemented. (This cobalt re-dissolution can occur by hydrogen evolution (corrosion) following the reaction $Co + 2H^+ = Co^{2+} + H_2$ or by cementation reaction of Ni^{2+} and Cu^{2+} ions onto formed metallic cobalt deposit by the formation of galvanic coupling by microcells (Ni and Cu more noble than cobalt) following the reactions $Ni^{2+} + Co = Co^{2+} + Ni$ and $Cu^{2+} + Co = Co^{2+} + Cu$. These phenomena might result in reducing the cementation process of cobalt [14–17,19].)

Whatever the acting parameter is, the fast initial period of nickel cementation observed after the transition period shows

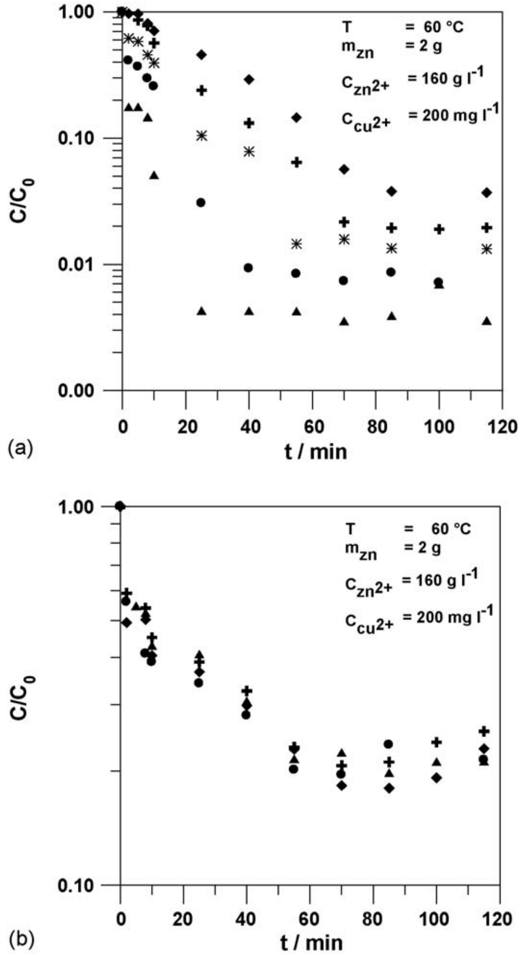

Fig. 2. Typical log (C/C_0) vs. time at different stirring rate: (a) nickel and (b) cobalt (♦) 101; (✚) 142; (✳) 228; (●) 468 and (▲) 1048 rad s^{-1}.

that the product of the mass transfer coefficient by the effective surface area follows Eq. (1).

The analysis of Fig. 2 makes evident that the time for reaching best results of simultaneous cementation of cobalt and nickel is defined as 50–60 min. Also, it is clear that the most important and regular period for the cementation of nickel and cobalt corresponds to the one being just after the transition period. Therefore, the acting parameter on kinetic cementation of cobalt and nickel and the global mass transfer in the cell were investigated for these conditions.

For the bath reactor used in the present work, the product $\bar{k}a_e$, of the overall mass transfer coefficient $\bar{k}$ and the effective surface area a_e was calculated from the dynamic equation:

$$\bar{k}a_e = -\frac{2.3}{t}\log\frac{C}{C_0} \qquad (1)$$

A distinction has to be made between the two terms a and a_e representing specific geometrical surface area and specific effective surface, respectively [14,17,18]. It is not possible to know the value of a_e. However, this is not a problem for design because, as shown by Eq. (1), $\bar{k}$ and a_e do not have to be known separately but only as the product $\bar{k}a_e$.

In the present work, the effect of the processing parameters was first presented upon the kinetic of the cementation dealing with the variation of the product $\bar{k}a_e$.

Then the mass transfer in the reactor is analysed by introducing an apparent mass coefficient transfer $\hat{k}$ which is defined by:

$$\hat{k} = \frac{\bar{k}a_e}{a} \qquad (2)$$

The values of $\bar{k}a_e$ obtained from the slopes of straight lines in the log (C/C_0) versus time plots using Eq. (1), are plotted in Fig. 3 versus the stirring rate at different temperatures. The diffusion controlled nature of the nickel cementation process was confirmed by the fact that the product $\bar{k}a_e$ increases systematically with increasing stirring rate (Fig. 3a). The data fit the equation:

$$\bar{k}a_e = \text{cste}\ \Omega^{1.18} \qquad (3)$$

It can be observed also (Fig. 3b) that the stirring rate has no effect on the cobalt cementation rate suggesting that the reaction is chemically rate limited.

Fig. 4a and b show the variation of Arrhenius law giving the product $\bar{k}a_e$ for nickel and cobalt as a function of temperature at different stirring rate. The slopes of these plots yield to an activation energy of 80 ± 3 and 13 kJ mol^{-1} for cobalt and nickel,

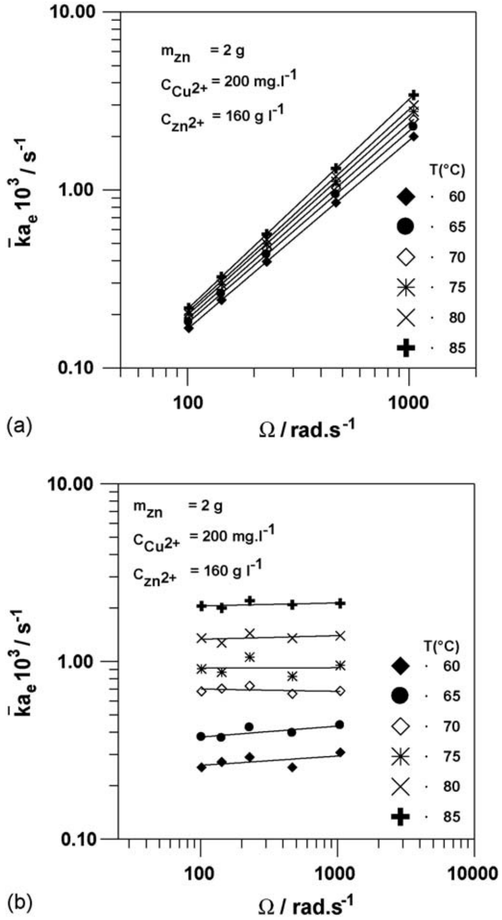

Fig. 3. Variation of $\bar{k}a_e$ as a function of stirring rate at different temperatures: (a) nickel and (b) cobalt.

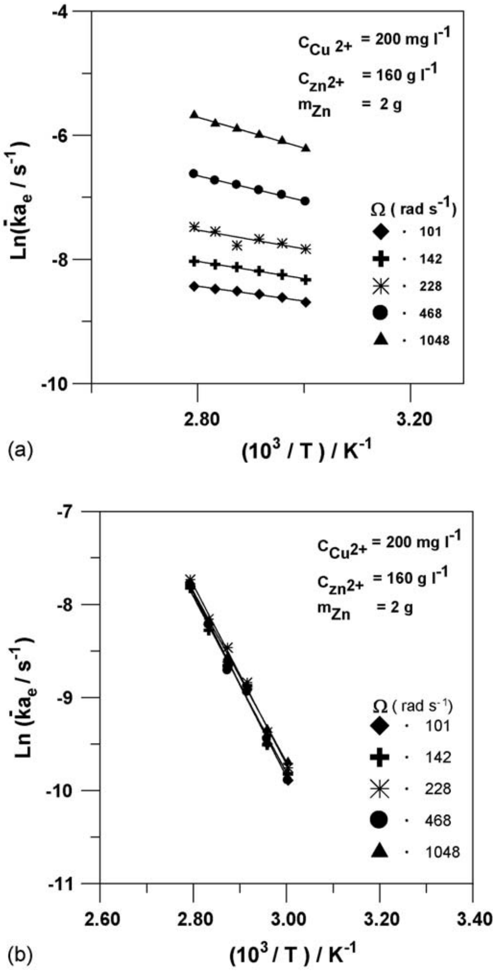

Fig. 4. Arrhenius plot of the experimental results: (a) nickel and (b) cobalt.

respectively, confirming that the reactions of cobalt and nickel are indeed under chemical and diffusion control, respectively.

It has been established that the presence of copper in the solution, which is used as cementation aids, is necessary for the antimony dissolution and cobalt cementation [19–24]. The effect of the copper concentration on the kinetic cementation rate is represented in Fig. 5. It is clear that the adding of copper activates to a greater extent the cementation of nickel (Fig. 5a) and to a smaller extent the cementation of cobalt (Fig. 5b). In the narrow copper concentration range used here, Fig. 5 also indicates that the cementation rate increased sensibly for the copper concentration ranged between 100 and 200 mg l^{-1} and remains nearly unchanged for the concentration going from 200 to 300 mg l^{-1}.

Fig. 6 shows the relation between product $\bar{k}a_e$ for different zinc dust quantity. It is observed that the kinetic of simultaneous cementation rate of nickel and cobalt is independent of zinc dust quantity, i.e., the specific geometric surface area of the reaction has no measurable effect on the mass transfer operation. From the percent recovery (Fig. 7) corresponding to experiment's time of 60 min, we can see that when the zinc dust is in quantities of 10–30 multiple surplus over the stoichiometric necessary quantity for cementation of copper, cobalt and nickel, then val-

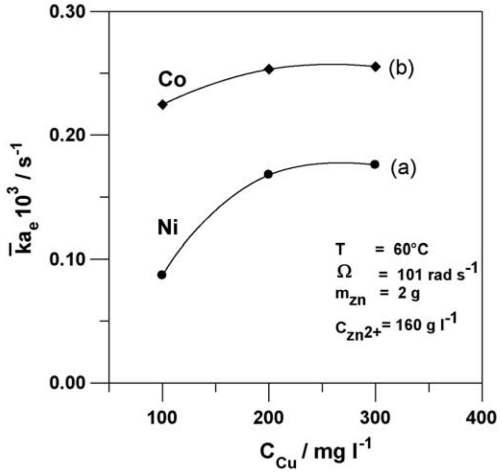

Fig. 5. Influence of copper content on simultaneous cobalt and nickel cementation: (a) nickel and (b) cobalt.

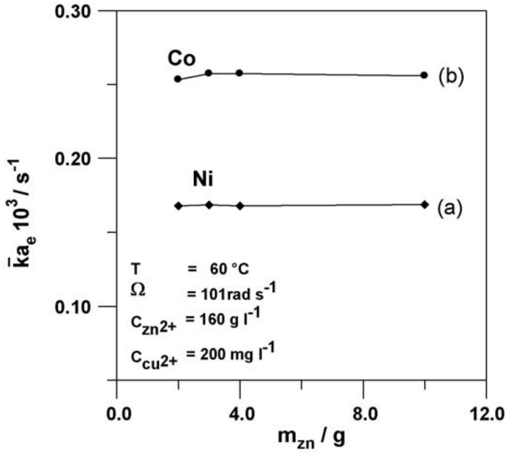

Fig. 6. Influence of zinc dust quantity on simultaneous cementation of cobalt and nickel: (a) nickel and (b) cobalt.

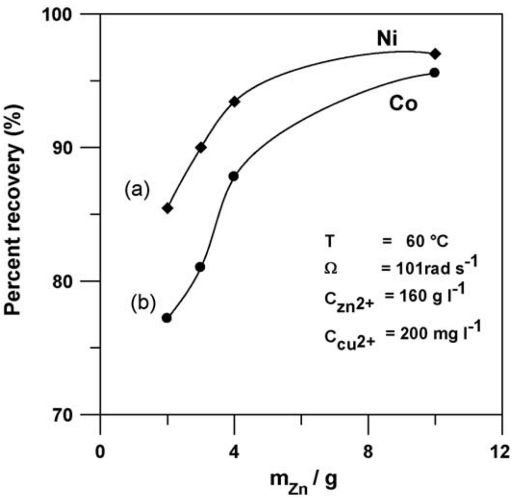

Fig. 7. Recovery of cobalt and nickel ions as a function of zinc dust quantity: (a) nickel and (b) cobalt.

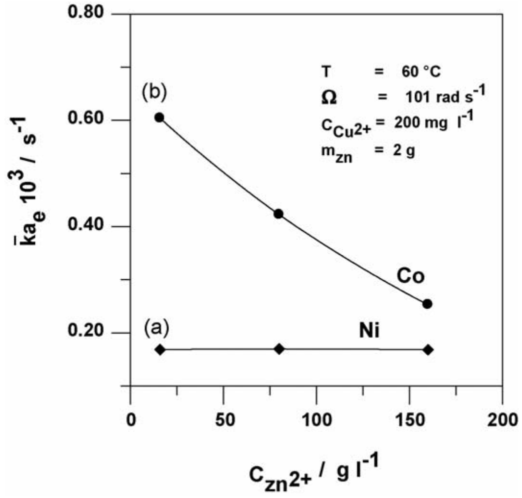

Fig. 8. Influence of zinc concentration on simultaneous cementation of cobalt and nickel: (a) nickel and (b) cobalt.

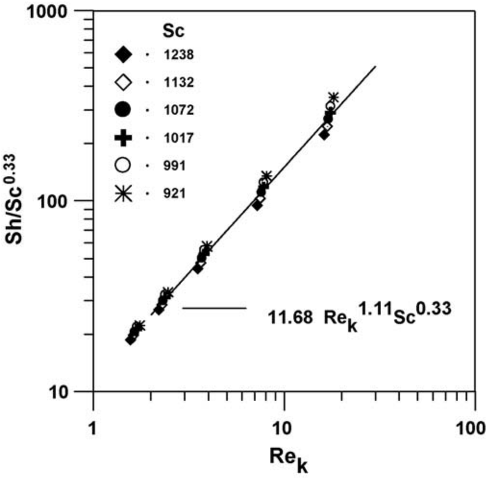

Fig. 9. Experimental data-mass transfer correlation.

ues of the percent recovery of cobalt and nickel are achieved that meet requirements for a solution which is to undergo electrolysis.

We can conclude from the results obtained in Fig. 8 that concentration of zinc ions plays an important role for the cementation of cobalt and negligible one for the cementation of nickel. This assumes that the zinc sulphate solution influences negatively the cementation of cobalt and it happens most probably through adsorption of Zn^{2+} ions on the surface of zinc powder thus making it effectively passive [1,23].

3.2. Mass transfer correlation and comparison

In order to evaluate the hydrodynamic effect over the global mass transfer in the stirring bath reactor, empirical correlation was envisaged using the dimensionless groups, *Sh*, *Re* and *Sc* which are often used to correlate mass transfer data in agitated system. The average diameter of particles was used as the characteristic length in calculating both *Re* and *Sh* numbers. As reported by Specchia et al. [25], there is a general agreement that the dependence of mass transfer coefficient on the Schmidt number can be described by *Sh* proportional to $Sc^{0.33}$ at a solid surface. Accordingly, this dependence is introduced in the following proposed correlation (4). Fig. 9 shows that, for the conditions $921 \leq Sc \leq 1238$ and $1 < Re_k < 20$, the calculated apparent mass transfer coefficient was plotted as *Sh* number against Reynolds. The data can be correlated by the equation:

$$Sh = 11.68 Re_k^{1.1} Sc^{0.33} \tag{4}$$

with standard deviation of ±0.51.

The results obtained in our stirred tank reactor system denote a highly turbulent flow as explained above regarding exponent of Reynolds number.

In order to compare our experimental results with those of literature, it is recommended to correlate them under analogous form ($(Sh-2)/Sc^{0.33} = \text{cste}\ Re_k^{a'}$) that is proposed by the authors [16,26–31], as a matter of fact, Eq. (4) may be written by alternate equation as follows:

$$\frac{Sh-2}{Sc^{0.33}} = 1.13 Re_k^{1.12} \tag{5}$$

For comparison, Fig. 10 presents different empirical correlations of literature [16,27,28,30,31]. It has been realized that our proposed correlation is systematically above the cited ones. The same remarks have been established by Alemany [26]. This difference appears to be linked to the increase in the surface area or/and from the presence of turbulence associated with increasing roughness of the deposit in addition to the fact that the true area of the rough particles (a_e) is higher than the geometrical area used (a) in calculating of the apparent mass transfer coefficient. The high value of the exponent of Reynolds (1.12) and the multiplicative coefficient (1.13) seen in Eq. (5) agree with the existence of turbulent flow near the deposit surface promoted by the increase of the surface roughness of the deposit [8,14,26].

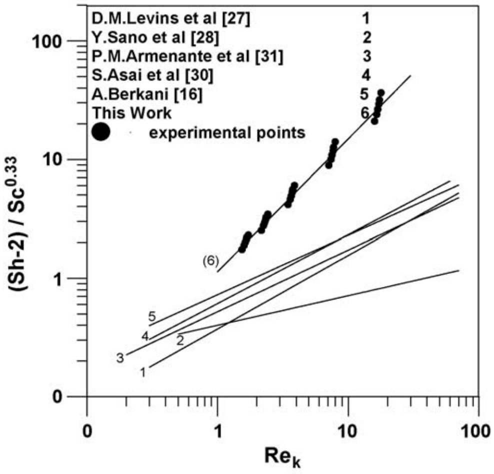

Fig. 10. Comparison of our experimental results with those of literature.

4. Conclusion

The cementation reaction of nickel was found to proceed with two different rates: an initial fast rate followed by a final slower one. The product $\overline{k}a_{\mathrm{e}}$ was calculated and the values increased with stirring rate and less affected by temperature. Mechanistic study of the reaction through activation energy determination ($13\,\mathrm{kJ\,mol^{-1}}$) showed that the cementation of nickel on zinc is a diffusion controlled reaction according to the following equation:

$$Sh = 11.68 Re_k^{1.1} Sc^{0.33}$$

where *Sh* is Sherwood number, *Sc*, Schmidt number and *Re* is Reynolds number.

The cobalt cementation results show the reverse dissolution of metallic cobalt cemented after 50 min of reaction. The cementation rate of cobalt was found first order reaction under chemical control.

The zinc sulphate concentration has no measurable effect on the kinetic cementation rate of nickel; however, it influences negatively the cementation of cobalt.

The lowest values of cobalt content have been obtained at a temperature of 85 °C and it was proved that the cobalt and nickel precipitation is optimum at copper concentration of $200\,\mathrm{mg\,l^{-1}}$.

References

[1] B. Boyanov, V. Konareva, N. Kolev, Removal of cobalt and nickel from zinc sulphate solutions using activated cementation, J. Min. Metall. 40B (1) (2004) 41–55.

[2] B. Boyanov, V. Konareva, N. Kolev, Purification of zinc sulfate solutions from cobalt and nickel trough activated cementation, Hydrometallurgy 73 (2004) 163–168.

[3] L. Muresan, G. Maurin, L. Oniciu, D. Gaga, Influence of metallic impurities on zinc electrowinning from sulphate electrolyte, Hydrometallurgy 43 (1996) 345–354.

[4] V. Karoleva, Metallurgy of Non-Ferrous Metals, vol. 2, Technika, Sofia, 1986 (in Bulgarian).

[5] A. Fontana, R. Winand, Contribution à l'étude de la cémentation du cobalt par du zinc métallique en vue de purifier les solutions utilisées pour la production du zinc électrolytique, Metallurgie XI-3 (1971) 162–167.

[6] P.H. Strickland, F. Lawson, The measurement and interpretation of cementation rate data, in: Proceeding of the International Symposium on Hydrometallurgy, New York, 1973, pp. 293–329.

[7] M. Karavastera, The effect of certain surfactants on the cementation of nickel from zinc sulphate solutions by suspended zinc particles in the presence of copper, Can. Metall. Q. 38 (3) (1999) 207–210.

[8] A. Dib, L. Makhloufi, Mass transfer correlation of simultaneous removal by cementation of nickel and cobalt from sulfate industrial solution containing copper. Part I: onto rotating zinc electrode disc, Chem. Eng. J., submitted for publication.

[9] V. Annamalai, J. Hiskey, L. Murr, The effects of kinetic variables on the structure of copper deposits cemented on pure aluminum discs: a scanning electron microscopic study, Hydrometallurgy 3 (1978) 163–180.

[10] V. Annamalai, L. Murr, Influence of deposit morphology on the kinetics of copper cementation on pure iron, Hydrometallurgy 4 (1979) 57–82.

[11] M.T. Oo, T. Tran, The effect of lead on the cementation of gold by zinc, Hydrometallurgy 26 (1) (1991) 61–74.

[12] E.C. Lee, F. Lawson, K.N. Han, Effect of precipitant surface roughness on cementation kinetics, Hydrometallurgy 3 (1978) 7–21.

[13] R.M. Nadkarni, M.E. Wadsworth, A kinetic study of copper precipitation on iron. Part II, Trans. Met. Soc. AIME 239 (1967) 1066–1074.

[14] A. Dib, L. Makhloufi, Cementation treatment of copper in wastewater: mass transfer in a fixed bed of iron spheres, Chem. Eng. Process. 43 (2004) 1265–1273.

[15] Y. EL-Tawil, Cementation of cupric ions from copper sulphate solution using fluidized bed of zinc powder, Z. Metallkde H8 (1988) 544–547.

[16] A. Berkani, Etude de la cémentation du cuivre par la poudre de zinc en réacteurs agités, Doctorat Thesis, I.N.P.G, Grenoble, France, 1992.

[17] K. Kubo, A. Mishima, Copper recovery from wastewater by cementation utilizing packed bed of iron spheres, J. Chem. Eng. Jpn. 12 (6) (1979) 495–497.

[18] S. Langlois, F. Coeuret, Flow-trough and flow-by porous electrodes of nickel foam. II. Diffusion-convective mass transfer between the electrolyte and the foam, J. Appl. Electrochem. 19 (1989) 51–60.

[19] A. Fontana, J. Martin, J. Van Severen, R. Winand, IIème Partie. Influence d'autres impuretés, Metallurgie XI-3 (1971) 168–179.

[20] O. Bockman, T. Ostvold, Products formed during cobalt cementation on zinc in zinc sulfate electrolytes, Hydrometallurgy 54 (2000) 65–78.

[21] O. Bockman, T. Ostvold, The influence of tartrate on cobalt cementation on a rotating zinc disc in zinc sulphate, Hydrometallurgy 55 (2000) 107–112.

[22] G. Nassef, Method for purification of zinc sulfate solutions. Canadian Patent 1046288, C22B19/26 (1975).

[23] A. Nelson, G.P. Demopoulos, G. Houlachi, The effect of solution constituents and novel activators on cobalt cementation, Can. Metall. Q. 39 (2) (2000) 175–186.

[24] G. Owuzu, Oxidation–precipitation of Co from Zn–Cd–Co–Ni sulphate solution using Caro's acid, Hydrometallurgy 48 (1) (1998) 91–99.

[25] V. Specchia, G. Baldi, A. Gianetto, Solid–liquid mass transfer in cocurrent two-phase flow trough packed beds, Ind. Eng. Chem. Process. Des. Dev. 17 (1978) 362–367.

[26] C. Alemany, Etude de l'influence du dépôt et de la surface active sur la cinétique de cémentation: d'une configuration hydrodynamique maîtrisée, l'électrode à disque tournant, à la poudre en réacteur agité, Doctorat Thesis, INPG, Grenoble, France, 1998.

[27] D.M. Levins, J.R. Glastonbury, Particle-liquid hydrodynamics and mass transfer in a stirred vessel. PartII-mass transfer, Trans. Inst. Chem. Eng. 50 (1972) 132–145.

[28] Y. Sano, N. Yamaguchi, T. Adachi, Mass transfer coefficients for suspended particles in agitated vessels and bubble columns, J. Chem. Eng. Jpn. 7 (4) (1974) 255–261.

[29] R. Kuboi, I. Komasowa, T. Otake, M. Iwasa, Fluid and particle motion in turbulent dispersion-III: particle–liquid hydrodynamics and mass-transfer in turbulent dispersion, Chem. Eng. Sci. 29 (1974) 659–668.

[30] S. Asai, Y. Konishi, Y. Sasaki, Transfer between fine particles and liquids in agitated vessels, J. Chem. Eng. Jpn. 21 (2) (1988) 107–112.

[31] P.M. Armenante, D.J. Kirwan, Mass transfer to microparticles in agitated systems, Chem. Eng. Sci. 44 (12) (1989) 2781–2796.